

Supporting Information

Serum Protein Resistant Behavior Of Multisite-Bound Poly(Ethylene Glycol) Chains Onto Iron Oxide Surfaces

Nicoletta Giambianco^{*}, Giovanni Marletta^{*}, Alain Graillot, Nicolas Bia, Cédric Loubat and Jean-François Berret^{*}

- Figure S1** – Polymer synthesis
 - Figure S2** – Polymer characterization
 - Figure S3** – Polymer acid-base titration
 - Figure S4** – NMR characterization
 - Figure S5** – Iron oxide nanoparticle characterization
 - Figure S6** – Stability in physiological and culture media
 - Figure S7** – QCM-D of phosphonic acid poly(ethylene glycol) copolymers on Fe₃O₄ substrates
 - Figure S8** – Binding kinetics for phosphonic and carboxylic acid PEG copolymers on iron oxide substrate at pH 2.0 and pH 7.4 as determined by QCM-D
 - Figure S9** – Binding kinetics for phosphonic acid PEG copolymers as a function of the molecular weight
 - Table S1** – Estimation of the polymer areal mass density using the Voigt model
-

Supporting Information Figure S1 – Polymer synthesis

Poly(PEGMA-co-MAPC1) copolymer was first synthesized by free radical polymerization involving PEGMA and MAPC1 monomers, AIBN as radical initiator and methylethylketone (MEK) as solvent. (Figure S1). Typical polymerization procedure is described here in the case of PEGMA_{1K} (950 g/mol) : MAPC1 (6.57 g, 32 mmol), PEGMA_{1K} (30 g, 32 mmol), AIBN (0.36g, 2.2 mmol) were added along with 60 mL MEK in a Schlenk flask. The mixture was degassed by three freeze–evacuate–thaw cycles and then heated at 75 °C under argon in a thermostated oil bath for 24 hours leading to 100% conversion. Poly(PEGMA-co-MAPC1) statistical copolymer was recovered after evaporation of the solvents under reduce pressure.

The second step corresponding to the hydrolysis of the phosphonated ester into phosphonic acid (Figure S1, bottom) was performed using bromotrimethylsilane and then methanol at room temperature as already reported in the literature (see for instance: A. Graillet *et al.*, *Polymer Chemistry* 2013, 4, 795-803; B. Canniccioni *et al.*, *Polymer Chemistry* 2013, 4, 3676-3685). Final polymer was finally recovered after 3 precipitations in diethyether.

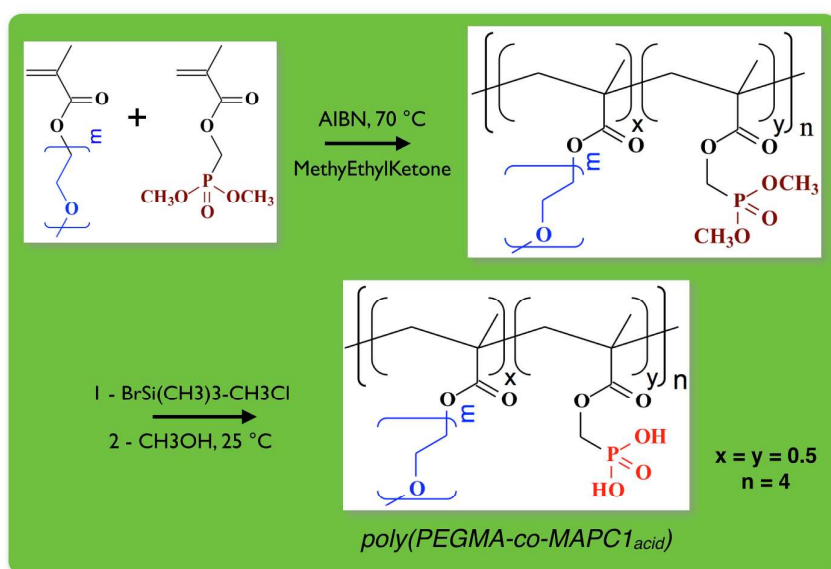


Figure S1: Two-step synthesis of poly(poly(ethylene glycol) methacrylate-co-dimethyl(methacryloyloxy)methyl phosphonic acid), abbreviated as poly(PEGMA-co-MAPC1_{acid}) and described as phosphonic acid PEG copolymer.

Supporting Information Figure S2 – Polymer characterization

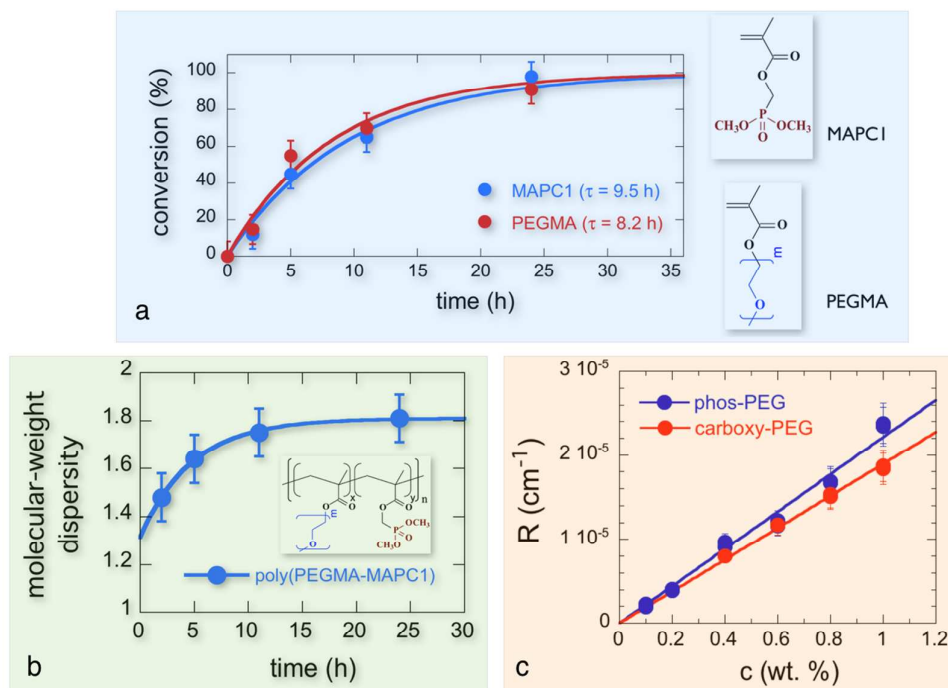


Figure S2: a) Percentage of the monomer conversion as a function the time for poly(PEGMA-co-MAPC1) copolymers. The continuous lines are best fit calculation using an exponential growth function. The characteristic times are indicated in the legend. b) Index of polymolecularity of poly(PEGMA-co-MAPC1) copolymers synthesized by free radical polymerization as a function of the synthesis time. The continuous line is a guide for the eyes. c) Rayleigh ratios of polymer solution as a function of the concentration determined by static light scattering measurements using a NanoZS Zetasizer from Malvern Instrument. For the calculations of $\mathcal{R}(c)$, we used $n_0 = 1.333$, $n_T = 1.497$ and $\mathcal{R}_T = 1.352 \times 10^{-5} \text{ cm}^{-1}$ at $\lambda = 633 \text{ nm}$. The molecular weight of the polymer was derived from the Zimm representation ($Kc/\mathcal{R}(c)$ versus the concentration c), using a scattering constrast $K = 1.5 \times 10^{-7} \text{ cm}^2 \text{ g}^{-2}$.

Supporting Information Figure S3 – Polymer acid-base titration

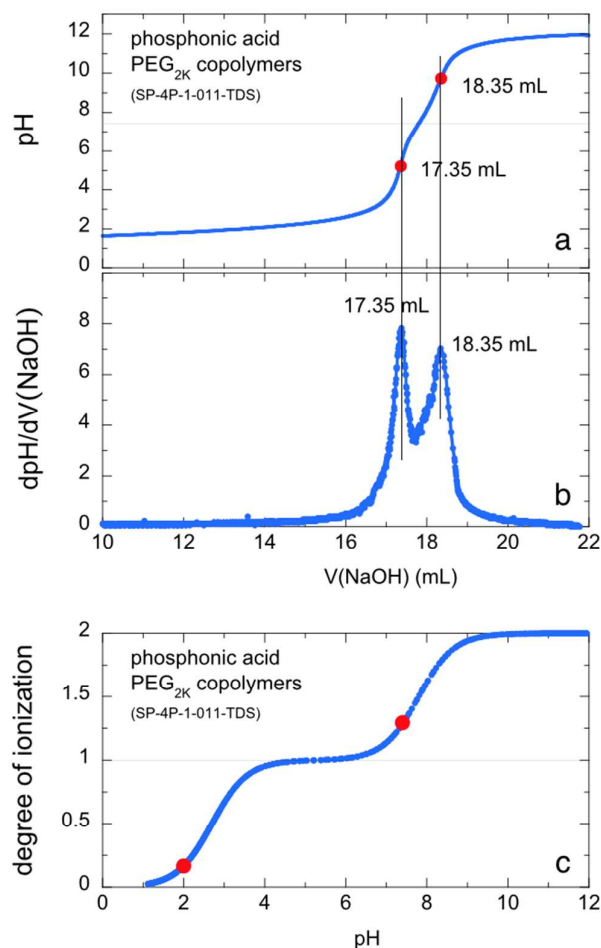


Figure S3: Acid-base titrations of phosphonic acid PEG copolymer dispersion by sodium hydroxide solution. a) pH measured as a function the NaOH added volume. b) Derivative of the pH with respect to NaOH added volume. The volume difference between the two maxima is used to determine the number of phosphonic acid moieties per chain (Table I). c) Degree of ionization *versus* pH calculated from the $\text{pK}_{\text{A}1} = 2.7$ and $\text{pK}_{\text{A}2} = 7.8$ of phosphonic acid PEG copolymers.

Supporting Information Figure S4 – NMR characterization

Synthesized copolymers were characterized after both polymerization step and hydrolysis step. Corresponding chemical shifts are given below:

- poly(PEGMA-*co*-MAPC1)

^1H NMR (CDCl_3 , 300MHz) δ (ppm): 4.4-3.9 ($\text{O}=\text{C}-\text{O}-\underline{\text{C}}\text{H}_2-\text{CH}_2$, $\text{O}=\text{C}-\text{O}-\underline{\text{C}}\text{H}_2-\text{P}$), 3.9-3.7 ($\text{O}=\text{P}-(\text{O}\underline{\text{C}}\text{H}_3)_2$), 3,7-3,4 ($\underline{\text{C}}\text{H}_2-(\text{O}-\underline{\text{C}}\text{H}_2-\underline{\text{C}}\text{H}_2)_{n-1}-\underline{\text{C}}\text{H}_3$), 3.4-3.3 ($\text{CH}_2-(\text{O}-\underline{\text{C}}\text{H}_2-\text{CH}_2)_{n-1}-\underline{\text{C}}\text{H}_3$), 2.3-1.2 ($\text{C}(\underline{\text{C}}\text{H}_3)-\underline{\text{C}}\text{H}_2$), 1.1-0.6 ($\text{C}(\underline{\text{C}}\text{H}_3)-\text{CH}_2$). ^{31}P NMR (CDCl_3 , 300MHz) δ (ppm): 21.8 ppm
- poly(PEGMA-*co*-MAPC1_{acid})

^1H NMR (D_2O , 300MHz) δ (ppm) – See Figure S4: 4.3-3.8 ($\text{O}=\text{C}-\text{O}-\underline{\text{C}}\text{H}_2-\text{CH}_2$, $\text{O}=\text{C}-\text{O}-\underline{\text{C}}\text{H}_2-\text{P}$), 3.8-2.8 ($\underline{\text{C}}\text{H}_2-(\text{O}-\underline{\text{C}}\text{H}_2-\underline{\text{C}}\text{H}_2)_{n-1}-\underline{\text{C}}\text{H}_3$) 2.2-1.5 ($\text{C}(\underline{\text{C}}\text{H}_3)-\underline{\text{C}}\text{H}_2$), 1.4-0.2 ($\text{C}(\underline{\text{C}}\text{H}_3)-\text{CH}_2$). ^{31}P NMR (D_2O , 300MHz) δ (ppm): 18.1 ppm

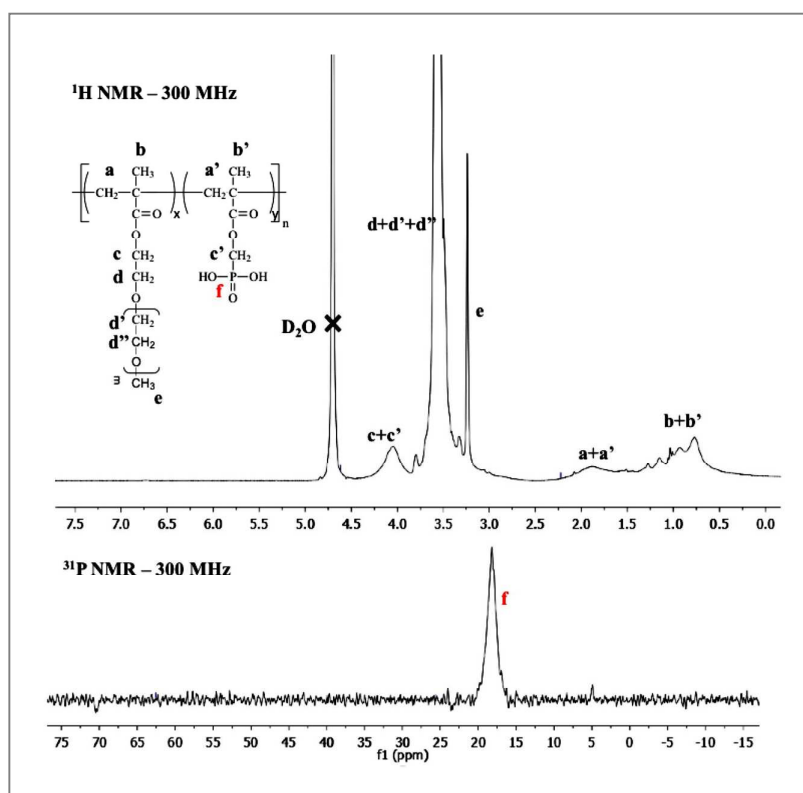


Figure S4: ^1H NMR and ^{31}P NMR characterization of Poly(PEGMA_{1K}-*co*-MAPC1)

The molar equivalent of acid groups per gram was determined after the polymerization step by ^1H NMR spectroscopy comparing the signal of the methyl end group at 3.4-3.3 ppm ($\text{CH}_2-(\text{O}-\underline{\text{C}}\text{H}_2-\underline{\text{C}}\text{H}_2)_{n-1}-\underline{\text{C}}\text{H}_3$) and the signal of the methylester phosphonate at 3.9-3.7 ppm ($\text{O}=\text{P}-(\text{O}\underline{\text{C}}\text{H}_3)_2$) (Figure S4). Comparison of both signals allows confirming the proportion of both monomers units into the polymers ($x = 0.5$ and $y = 0.5$). This was expected since (i) the monomers were introduced in same proportion in the reactive media and (ii) the monomers conversion reached 100%. Finally, knowing the molar amount of MAPC₁ (2 acidity per unit) per grams of polymers, it was possible to deduce the molar equivalent of acid groups per gram of polymers.

Supporting Information Figure S5 – Iron oxide nanoparticle characterization

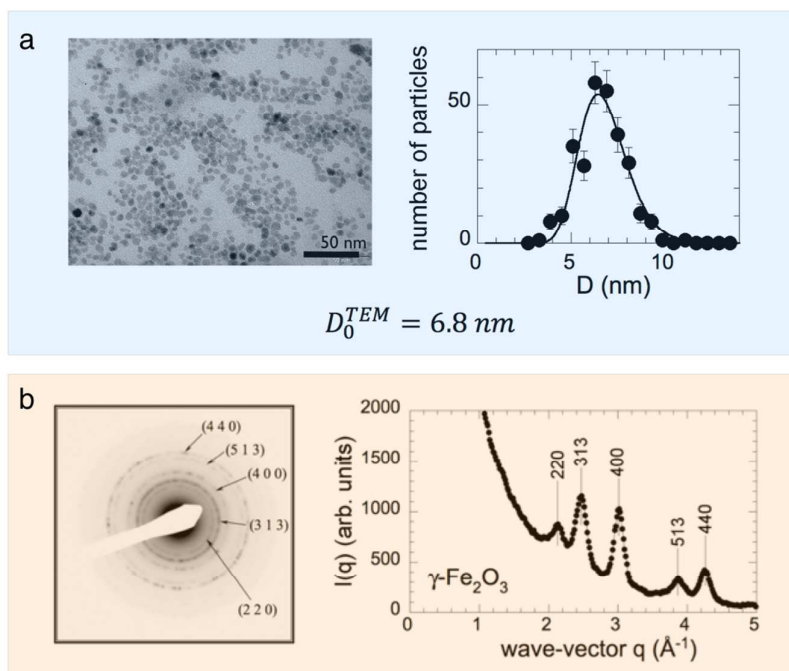


Figure S5: a) Images of transmission electron microscopy (TEM) of iron oxide nanoparticles at a 160000 \times magnification. TEM was carried out on a Jeol-100 CX microscope at the SIARE facility of University Pierre et Marie Curie (Université Paris-VI). On the right hand-side is the size distribution derived from TEM, together with a log-normal function of median diameter 6.8 nm and size dispersity 0.18. b) *left:* Microdiffraction pattern obtained from iron oxide nanoparticles. *right:* Corresponding wave-vector dependence of the scattering intensity.

Supporting Information Figure S6 – Stability in physiological and culture media

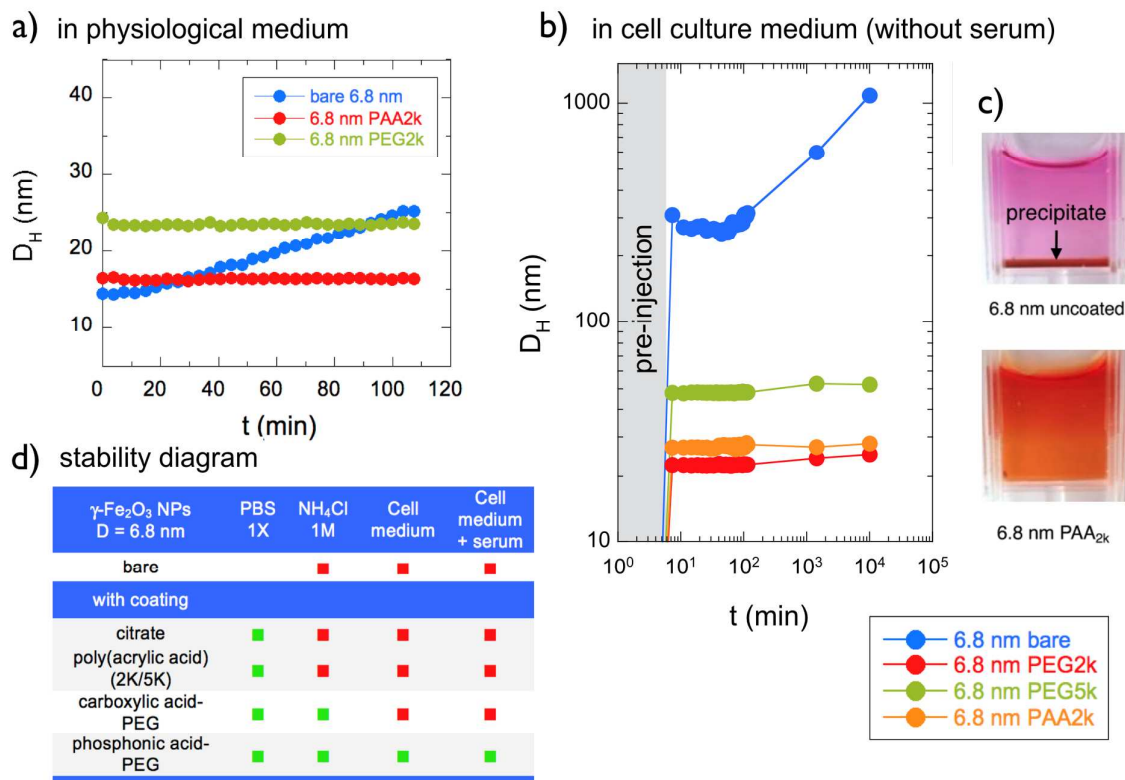


Figure S6: **a)** Hydrodynamic diameter D_H for bare and coated 6.8 nm iron oxide nanoparticles in physiological medium (PBS1X). The stability assays were performed at a weight concentration of 0.1 wt. %. **b)** Same as in a) using the Dulbecco's Modified Eagle's Medium (DMEM) without serum. The increase in D_H after the initial jump (which corresponds to the injection of the particles into the cell) is indicative of the dispersion destabilization. **c)** Images of iron oxide dispersions in DMEM after one week. **d)** Comparison of the colloidal stability of bare and coated 6.8 nm $\gamma\text{-Fe}_2\text{O}_3$ nanoparticles in various media. Green squares indicate that the particles are stable, red squares unstable.

Supporting Information Figure S7 – QCM-D of phosphonic acid poly(ethylene glycol) copolymers on Fe₃O₄ substrates

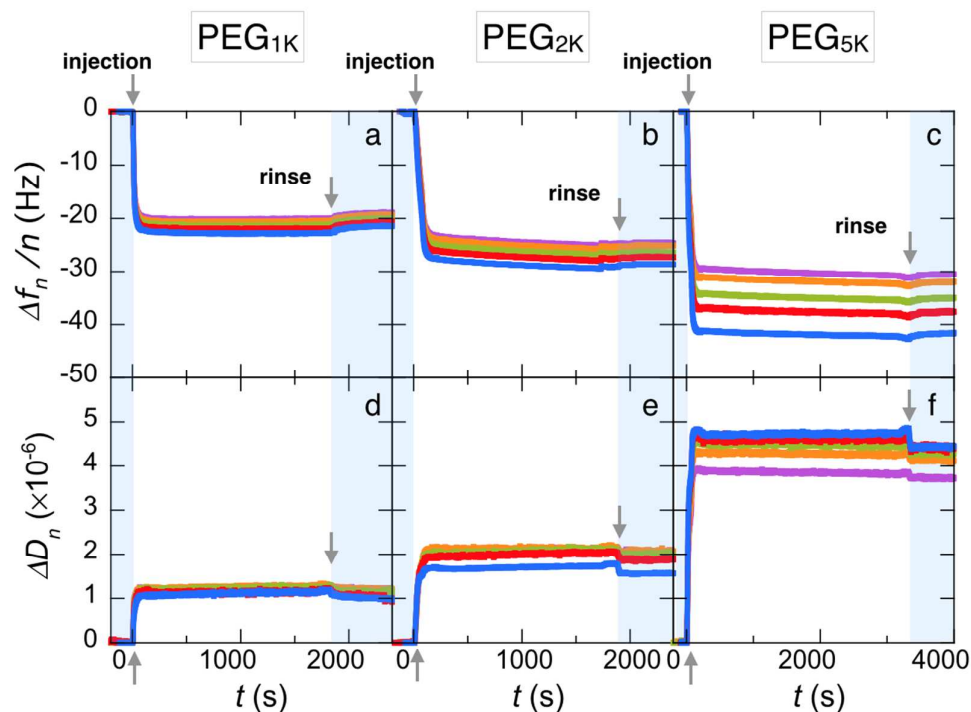


Figure S7: Binding curves for frequency $\Delta f_n/n$ and dissipation ΔD_n ($n = 3, 5, 7, 9$ and 11) following the injection of the polymer dispersion. The data for the third harmonics are shown in Figure 3 in the main text. In each panel, the first arrow at $t = 0$ denotes the time at which the polymer solution (concentration 0.1 wt. %) is injected. The second arrow denotes the time at which DI-water (pH 7.4) is introduced for rinsing.

Supporting Information Figure S8 – Binding kinetics for phosphonic and carboxylic acid PEG copolymers on iron oxide substrate at pH 2.0 and pH 7.4 as determined by QCM-D

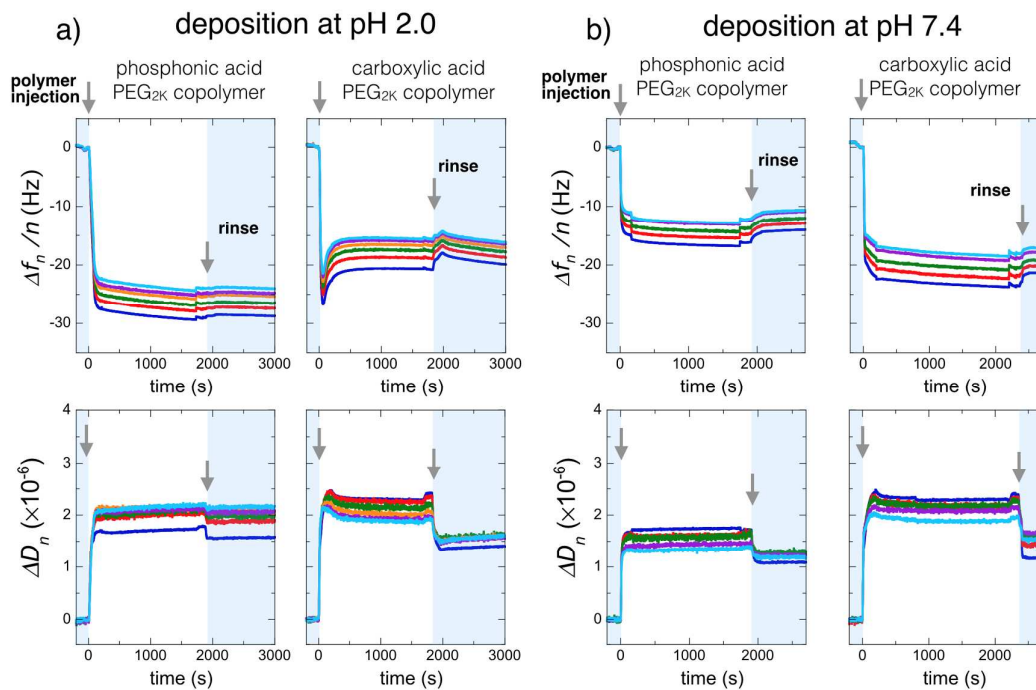


Figure S8: a) Binding curves for frequency $\Delta f_n/n$ and dissipation ΔD_n ($n = 3, 5, 7, 9$ and 11) following the injection of a polymer dispersion at pH 2.0. The data for the third harmonics are shown in Figure 4 in the main text. In each panel, the first arrow at $t = 0$ denotes the time at which the polymer solution (concentration 0.1 wt. %) is injected. The second arrow denotes the time at which DI-water (pH 7.4) is introduced for rinsing. b) Same as in a) for a polymer injection at pH 7.4.

Supporting Information Figure S9 – Binding kinetics for phosphonic acid PEG copolymers as a function of the molecular weight

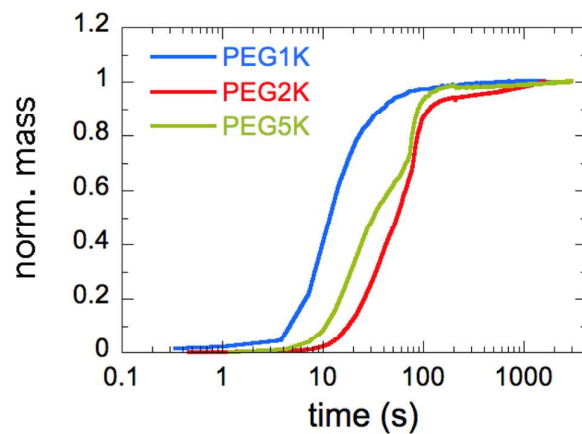


Figure S9: Normalized masses of PEG_{1K}, PEG_{2K} and PEG_{5K} phosphonic acid containing polymers deposited on Fe₃O₄ surface at pH 2. The data exhibits one linear stage for short PEG chains and two stages for the longer ones. The longer the polymer, the slower the adsorption. As the surface coverage increases, the adsorption process becomes faster for the longer PEG tether copolymer.

Supporting Information Table S1 – Estimation of the polymer areal mass density using the Voigt model

For a dense layer, the Voigt model predicts a relationship between the thickness and the frequency shift of the form: $h_{2D} \approx -m_q \Delta f / f \rho_f$ (J. Fang *et al.*, *Analyst* **140**, 1323 (2015)). Here h_{2D} is the layer thickness, m_q is the areal mass of the quartz sensor, Δf is the frequency shift, f the fundamental frequency (5 MHz) and ρ_f is the layer mass density. For polymeric films at solid-liquid interfaces, $\rho_f = 1.0 \text{ g cm}^{-3}$ is assumed. Under these conditions, a 1 Hz shift in frequency corresponds to a 0.17 nm change in thickness.

terminus	M_n (PEG) g mol ⁻¹	mass ng cm ⁻² from Δf	thickness h nm	mass ng cm ⁻² from Voigt model
phosphonic acid (pH 2.0)	1000	400	4.1	430
	2000	520	5.7	600
	5000	750	9.4	970
carboxylic acid (pH 2.0)	2000	370	4.6	480

Table S1: Comparison between the areal mass densities for phosphonic acid PEG copolymer deposition obtained from the Sauerbrey equation and from the Voigt model.

The agreement between the two determinations is fair. The discrepancies observed for carboxylic acid PEG_{2K} and phosphonic acid PEG_{5K} copolymers could be due to the fact that for these polymers the PEGs are not forming a dense layer. This later conclusion is in agreement with PEG number densities around 0.1 – 0.3 nm⁻² (Table 2). Two sentences have been added at the end of Section III.3